



## Curvature-based Penalty for Anatomical and Functional MR Human Spine Image Registration

Sahar Sabaghian<sup>1\*</sup>, Mohsen Soryani<sup>1\*</sup>, Mohammad Ali Oghabian<sup>2</sup>  
and Amir Hossein Batoli<sup>2</sup>

<sup>1</sup>*Iran University of Science and Technology, School of Computer Engineering, Iran.*

<sup>2</sup>*Tehran University of Medical Sciences, Iran.*

### *Authors' contributions*

*This work was carried out in collaboration between all authors. All authors read and approved the final manuscript.*

### *Article Information*

DOI: 10.9734/BJMCS/2016/25075

*Editor(s):*

(1) Victor Carvalho, Polytechnic Institute of Cávado and Ave, Portuguese Catholic University and Lusiada University, Portugal.

*Reviewers:*

(1) Hammad Khalil, University of Malakand, Pakistan.

(2) R. Gayathri, Sri Venkateswara College of Engineering, India.

(3) Anonymous, Universiti Sains, Malaysia.

(4) Yaoqin Xie, Shenzhen Institutes of Advanced Technology, Chinese Academy of Sciences, China.

Complete Peer review History: <http://sciencedomain.org/review-history/14503>

**Received: 17<sup>th</sup> February 2016**

**Accepted: 5<sup>th</sup> April 2016**

**Published: 7<sup>th</sup> May 2016**

**Original Research Article**

## Abstract

This paper describes an application of image registration. The method is based on an efficient implementation of the curvature registration. This non-rigid registration allows us to find best geometric correspondence between two images. The goal is to register anatomical and functional spine images of the same patient to localize functionality in anatomical images. Most of previous experiments have been tested on brain images and it is the first time that the variational method has been used to register spine images. Registration results are compared with those of MIRT toolbox using two kinds of similarity measures; mutual information (MI) and correlation ratio (CR). MIRT is a Matlab software package for 2D and 3D non-rigid image registration. The model of transformation is parametric and based on B-spline method. Superior results have been achieved compared to the results of MIRT.

*Keywords: Image registration; non-rigid deformation; spine images.*

\*Corresponding author: E-mail: [Sahar.Sabaghian@gmail.com](mailto:Sahar.Sabaghian@gmail.com), [Soryani@iust.ac.ir](mailto:Soryani@iust.ac.ir);

## 1 Introduction

Image registration is the process of finding the optimum geometrical transformation that seeks for the best corresponding points between two images. The image registration aligns one of the images, known as the template set (T) with another image which is the reference set (R). There are different types of registration methods such as rigid registration and non-rigid (deformable) registration. The rigid registration method considers only rigid structures and uses a specific matrix to find deformities like rotation and translation but deformable or non-rigid registration considers the changes that take place over the time in the soft tissues and does not need any specific matrix for transformation [1].

Among the applications of medical image registration, the registration of functional and anatomical images is very important and applicable because unlike structural images, functional magnetic resonance images (fMRI) do not have any detailed structural and anatomical information. Therefore, to analyze these kinds of images it is necessary to register them. This type of registration is known as multimodal registration due to different modalities used in acquiring images.

In recent years, different kinds of registration algorithms for medical imaging applications have been developed. Sotiras has evaluated Deformable Medical Image Registration [2]. Maes proposed a free form Image registration using mutual information for CT and MR images of the prostate [3]. Prummer introduced a technique to register multi-modal non-rigid 2D-3D CT thorax images [4]. A parametric method for non-rigid registration based on B-spline models can be found in [5]. Legaz has developed a non-rigid multimodal image registration for MRI and FMRI of brain in frequency domain [6]. A unified approach to fast image registration and a new curvature based registration technique as a non-parametric method has been provided by Fischer [7]. Andriy developed a registration toolbox based on parametric methods MIRT (Medical Image Registration Toolbox) [8]. Mitra used a spline-based non-linear diffeomorphism to register prostate images [9].

In this work, we consider the registration of anatomical images (MR) and functional images (fMR) of spine for the first time in order to obtain the best correspondences between two image sets. Result of the registration process is used to fuse information of MRI and FMRI and provide better analysis of patient's spine abnormalities for surgeons and neuroscience specialists. The method is based on an efficient implementation of variational image registration (non-parametric).

The method has been compared with a parametric method; MIRT is a free form deformation toolbox for 2D non-rigid image registration. The model of transformation is parametric and based on B-spline method. MIRT supports different Similarity Measures such as Mutual Information (MI), Residual Complexity (RC), Sum of Squared Differences (SSD), Sum of Absolute Differences (SAD) and Correlation Coefficient (CC).

We will show that the non-parametric method is more accurate than the parametric method for spine images according to the results presented in this paper.

## 2 The Proposed Method

### 2.1 Variational image registration

In this paper we have been prepared 2D images of spine from medical studies. MRI and FMRI are treated as reference (R) and template (T) images respectively. The registration process produces a displacement field  $\mathbf{u}: \mathbb{R}^2 \rightarrow \mathbb{R}^2$  that makes the transformed template image be similar to the reference image,  $T(\mathbf{X} - \mathbf{u}(\mathbf{X})) \approx R(\mathbf{X})$ , where  $\mathbf{u}(\mathbf{X}) = (u_1(\mathbf{X}), u_2(\mathbf{X}))^T$  and  $\mathbf{X}$  is the spatial position  $\mathbf{X} = (x_1, x_2) \in \mathbb{R}^2$ .

Most of the registration methods define an energy functional such as (1) which has to be minimized. Minimizing this energy functional can be done by computing derivatives of terms D and S of (1) and these

derivatives produce new equations in terms of the variational calculus. This group of registration methods is known as variational methods.

$$J[\mathbf{u}] = D[R, T; \mathbf{u}] + \alpha S[\mathbf{u}] \quad (1)$$

J is the energy functional which includes two important terms. The first term is D measures the distance between the deformed template image and the reference image. S is a penalty term which acts as a regularizer and determines the smoothness of the displacement field and keeps the functional energy in minimum state.  $\alpha > 0$  is a weight coefficient for the regularization term.

The distance measure D is chosen depending on the images. If the images are from different modalities, statistical-based measures like mutual information, MI, [10,11,12,13] and correlation ratio, CR, [14,15] are more appropriate. In this work CR and MI have been used and registration results have been compared.

### **2.1.1 Mutual information**

Mutual information is the most popular measure for multimodal registration. It has been successfully applied to several modalities such as MR, FMRI, CT and PET. We have two images X and Y as inputs and we treat them as random variables. Mutual information between X and Y is given by:

$$I(X, Y) = \sum_{i, j} P(i, j) \log \frac{P(i, j)}{P(i)P(j)} \quad (2)$$

$P(i, j)$  is joint probability density function of two images,  $P(i)$  is marginal probability density function of reference image and  $P(j)$  in marginal probability density function of template image.

### **2.1.2 Correlation ratio**

Another similarity measure which has been proposed in [15] and is inherited from probability theory is known as the correlation ratio. This measure, in addition to generality, takes into account proximity in the intensity space and it is robust for images that have low resolution and has attractive computing time. Correlation ratio is a functional dependence measure between X and Y which is defined as follows:

$$1 - \eta[Y | X] = \frac{1}{\partial^2} \sum_i \partial_i^2 P_x(i) \quad (3)$$

$$\partial^2 = \sum_j j^2 P_y(j) - m^2 \quad m = \sum_j j P_y(j) \quad (4)$$

$$\partial_i^2 = \frac{1}{P_x(i)} \sum_j j^2 P_y(j) - m^2 \quad m_i = \frac{1}{P_x(i)} \sum_j j P(i, j) \quad (5)$$

This measure is supposed to determine how well X (reference image, MRI) approximates Y (template image, FMRI).  $\eta_{yx}$  lies between 0 and 1 and  $\eta_{yx} = 1$  showing no variance in intensities of Y when mapping to intensities in X, and implies a unique mapping from X to Y. A value near 1 indicates a high functional dependence while a value near 0 indicates a low functional dependence. If the variance of intensities decreases, the correlation ratio between X and Y increases [14].

The regularization term S gives the smoothness to the displacement field. A displacement field is smooth if it has no harsh jumps in magnitude, which is displacement in pixel neighborhood change gradually [7].

Here we use the curvature term for S, which is given by the energy of second order derivative of u [7]:

$$\delta^{curv} [u] = \frac{1}{2} \sum_{L=1}^d \int_{\Omega} (\Delta u_L)^2 dx \quad (6)$$

## 2.2 Numerical treatment of the minimization problem

The numerical method for the minimization of the joint functional Eq. (1) is to compute the derivative of J[u] [16]:

$$J[\mathbf{u}] = D [\mathbf{R}, \mathbf{T}; \mathbf{u}] + \alpha S[\mathbf{u}] \quad (7)$$

The derivative of J[u] is:

$$f(x, \mathbf{u}(x)) + \alpha A[\mathbf{u}](x) = 0 \quad (8)$$

In (7) the distance measure D is defined as:

$$D = 1/2 \int (T(x-\mathbf{u}) - R(x))^2 dx \quad (9)$$

The derivative of this distance measure is called force field and is used to drive the deformation. The derivative of D with respect to u can be written as follows:

$$f(x, \mathbf{u}(x)) = (R(x) - T(x - \mathbf{u}(x))) \cdot \nabla T(x - \mathbf{u}(x)). \quad (10)$$

The derivative of the regularization term S in (6) as driven in [16] is:

$$A_{curv}[\mathbf{u}] = \Delta^2 \quad (11)$$

To solve the partial differential equation of (8) a time marching algorithm used here:

$$\partial_t \mathbf{u}^{k+1}(x, t) = f(x, \mathbf{u}^k(x, t)) + \alpha A[\mathbf{u}^{k+1}](x, t), \quad k \geq 0, \quad (12)$$

$\mathbf{u}^0 = 0$ , and a finite difference forward approximation for the derivative is used and equations have to be solved in each iteration step (k).

## 2.3 Implementation of the curvature registration

Our implementation is based on curvature registration [7]. To begin with, we introduce a time step  $\tau$  and the uniformly grid points to discretize the problem. The displacement field and regularization term in discretization form are defined as follows:

The derivative is approximated using finite differences,

$$u_L(X, \tau k) \approx (U_L^{k+1} - U_L^k) / \tau \quad (13)$$

$$\Delta^2 u_L(X, \tau k) \approx S^{curv} * U_L^k \quad (14)$$

$$S^{curv} = S^{diff} * S^{diff} \quad (15)$$

$S^{diff}$  is defined as stencil of Laplace operator in  $d=2$ .

$$S^{diff,2} = \begin{pmatrix} 0 & 1 & 0 \\ 1 & -4 & 1 \\ 0 & 1 & 0 \end{pmatrix} \quad (16)$$

Now we can rearrange Eq. (12) as:

$$(\mathbf{I}_n + \tau \alpha \mathbf{A}^{\text{curv}}) \mathbf{U}_L^{k+1} = \mathbf{U}_L^k - \tau \mathbf{F}_L^k, \quad L = 1, \dots, d, \quad (17)$$

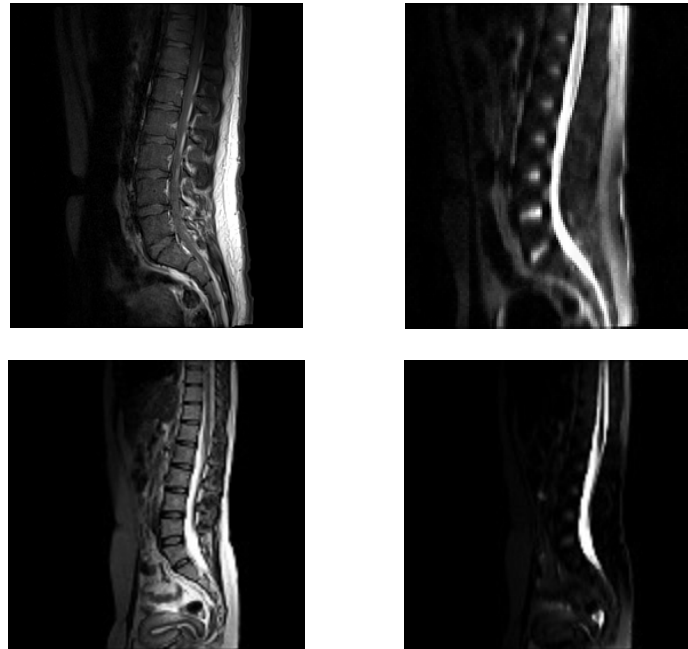
$\mathbf{I}_n$  is the identity matrix,  $\tau$  is time step and it depends on type of application.  $\alpha$  is a weighting coefficient for matrix  $\mathbf{A}$  and it depends on application too.  $\mathbf{U}_L^{k+1}$  is displacement field in the next step,  $\mathbf{U}_L^k$  is displacement field in the previous step and finally  $\mathbf{F}_L^k$  is the force field. The complexity of this equation is just calculation of matrix  $\mathbf{A}$ . this matrix is a tridiagonal matrix and represents the eigenvalues of discrete Laplace operator. Eq. (17) can be solved with DCT (discrete cosine transform) in a fast  $O(n \log n)$  implementation.

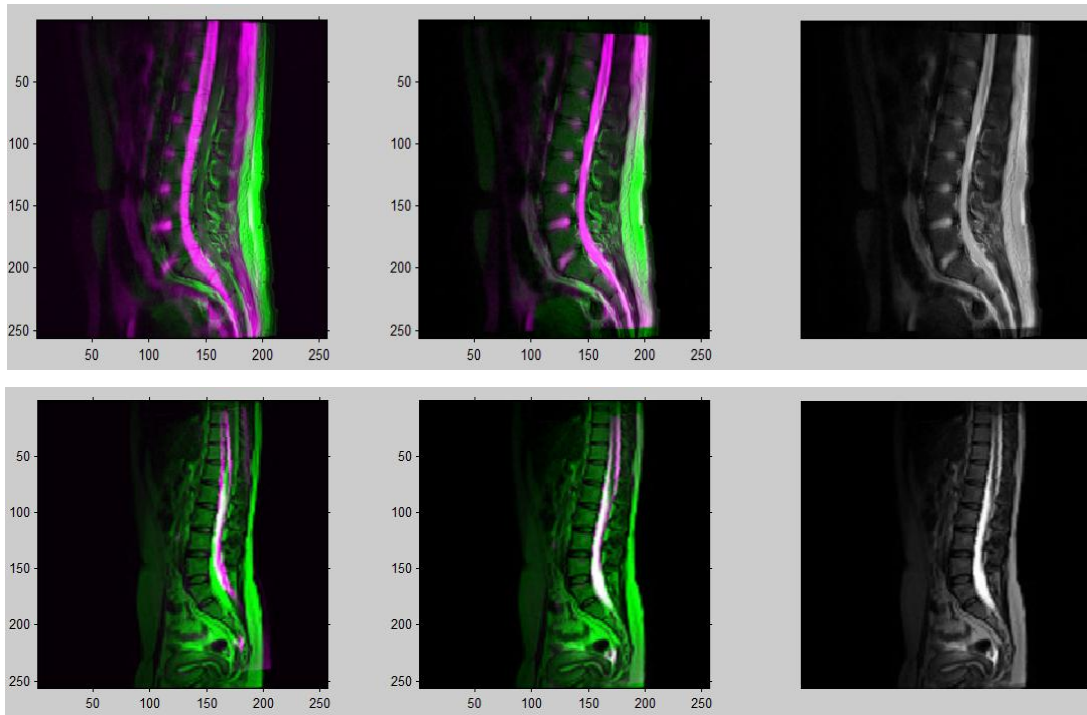
### 3 Experiments and Results

To illustrate the performance of the variational registration approach when applied to 2D human spine images we present results of registration for MRI and FMRI images taken from different views.

Fig. 1 shows the registration of images for sagittal view. The resolution of images is  $256 \times 256 \times 8$ . Parameters used for this view are  $\alpha = 200$ ,  $\tau = 2$  and algorithm implements for  $k = 200$  iterations. Looking at difference between MR and FMR images before and after registration in the third and fourth rows of this figure the positive effect of registration can be recognized.

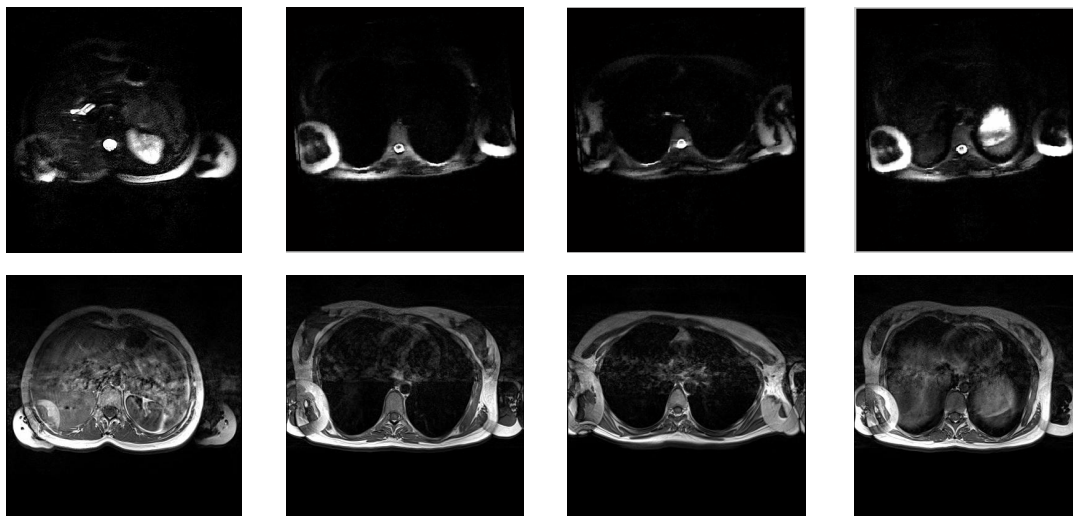
Fig. 2 shows the registration of spine images taken from axial view with  $256 \times 256 \times 8$  resolution. In this experiment template images have been translated 5 mm horizontally and rotated 5 degrees. Parameters used in this experiment are  $\alpha = 5$ ,  $\tau = 2$  and algorithm implements for  $k = 200$  iterations. Fusion between reference and registered template images using MI are shown in the third row and fusion between reference and registered template images using CR are shown in the fourth row.





**Fig. 1. Registration of MR and FMR images of spine for sagittal view (256\*256) using CR. First row from left: MR and FMR images of case1. Second row: MR and FMR images of case 2. Third row: difference before registration, difference after registration and fusion between reference and registered template images of the first row. Fourth row: Difference before registration, difference after registration and fusion between reference and registered template images of the second row**

In another experiment the FSL software was used to analyze the FMR image. The analyzing matrix and activation region were found. Then this information was superimposed on the MR as reference image before and after registration. The resolution of images is 256\*256\*8. Results of this experiment are shown in Fig. 3.



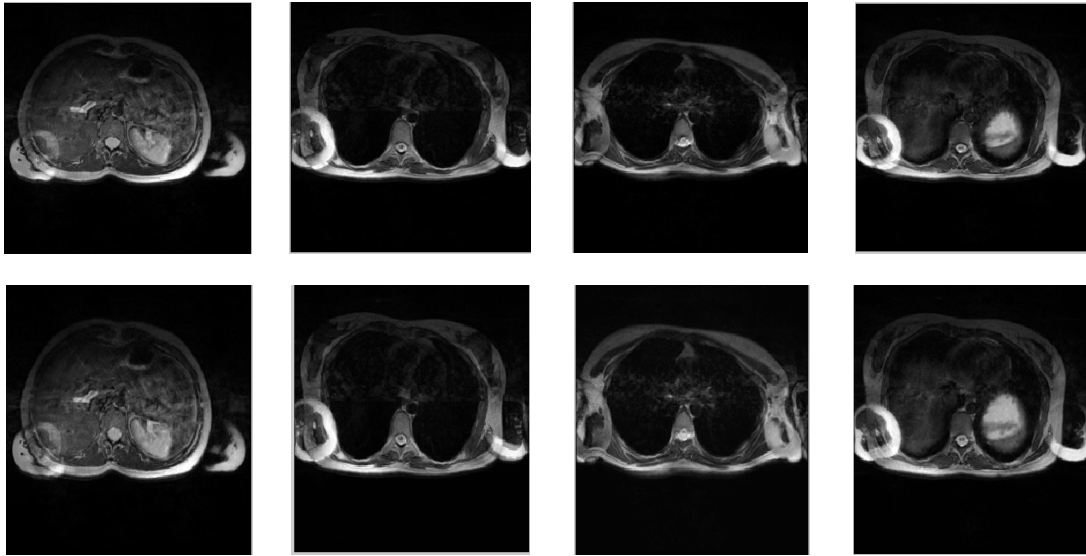


**Fig. 2. Registration of MR and FMR images of spine from axial view (256\*256\*8) for 4 different cases; first row: FMR template images, second row: MR reference images, third row: Fusion between reference and registered template images using MI, fourth row: Fusion between reference and registered template images using CR**



**Fig. 3. Results of applying the analyzing matrix on the registered image. First row from left: registration of MRI and FMRI (haste protocol), second row: superimposing the activation points on the reference image before and after registration**

Numerical measurements of the variational registration method for both similarity measures (MI & CR) for the first experiment (sagittal view) and comparison with the results of MIRT toolbox have been gathered in Table 1. Similar results and comparisons for the axial view have been shown in Table 2. As can be seen, the variational non-parametric registration method produces better results in terms of accuracy and time for these images for both similarity measures.

Results of the registration method for two noisy images were also produced and are shown in Tables 3 and 4. From these tables it can be concluded that the MI measure produces better results when the images have good quality and the CR measure is more suitable for noisy images. Because Figs. 4 and 5 are noisy images and the results for noisy images in Tables 3 and 4 show that CR works better than MI. Therefore we only show the results using CR. Sagittal and axial views of the noisy images for this experiment are shown in Figs. 4 and 5.



**Fig. 4. Registration of MR and noisy FMR images of spine from sagittal view (128\*128\*8); from left MR reference image, FMR template image and result of the fusion between reference and registered template images using CR**

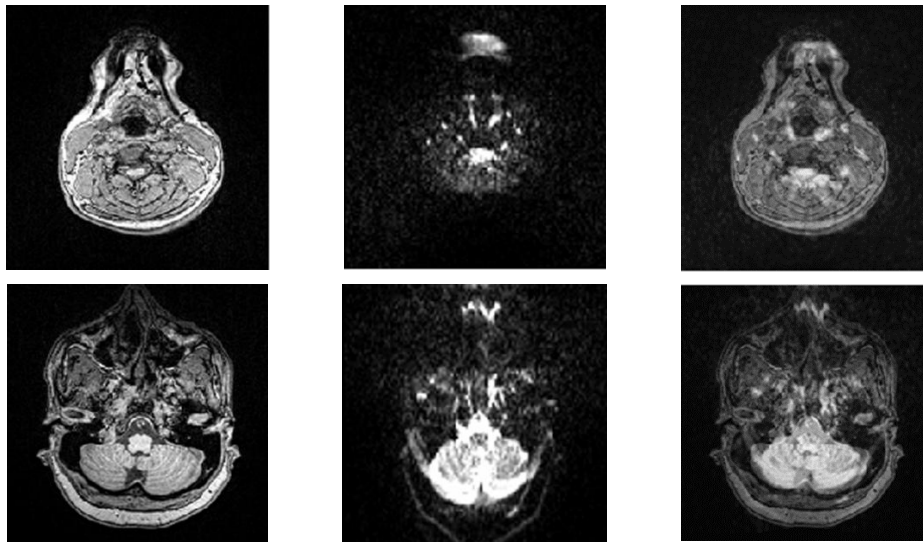


**Fig. 5. Registration of MR and noisy FMR images of spine from axial view for 2 samples; from left: MR reference image (220\*176\*8), FMR template image (110\*110\*8) and result of fusion between reference and registered template images (128\*128\*8) using CR**



**Table 1. Similarity measures computed for Sagittal view**

Case #	Non-parametric method (Variational method)							Parametric method (MIRT)						
	CR			MI				MI(space=1)			MI(space=5)			
	CR-bef	CR-Aft	Time(s)	MI	MI-Bef	MI-Aft	Time(s)	CR	MI-Aft	Time(s)	CR	MI-Aft	Time(s)	CR
1	0.53	0.72	14	744.5	422.9	751.6	9	0.72	753.2	124	0.75	748.6	6	0.72
2	0.54	0.73	14.7	760.2	443.4	774.5	8	0.74	780.5	134	0.76	753.7	11	0.73
3	0.55	0.74	14.7	772.5	446.7	786.2	9	0.74	777.3	168	0.76	734.7	9	0.74
4	0.56	0.73	14.8	794.7	449.3	810.4	12.4	0.74	798.5	205	0.75	809.7	11	0.74
5	0.55	0.73	14.6	851.4	437.0	828.4	8	0.74	807.7	122	0.74	824.4	12	0.73
6	0.56	0.75	14.1	835.3	446.4	834.8	13	0.76	813.1	161	0.77	811.9	13.2	0.75
7	0.56	0.76	14.1	841.3	437.8	804.3	17	0.76	801.5	166	0.77	799.8	13.3	0.75
8	0.55	0.71	14.5	770.2	432.5	806.9	9	0.74	782.8	174	0.75	802.7	12	0.73
$\mu$	0.55	0.73	14.4	<b>796.2</b>	439.5	<b>799.9</b>	10.6	0.74	<b>789.3</b>	156.7	0.74	<b>785.1</b>	10.9	0.73

**Table 2. Similarity measures computed for Axial view**

Case #	Non-parametric method (Variational method)							Parametric method (MIRT)						
	CR			MI				MI(space=1)			MI(space=5)			
	CR-bef	CR-Aft	Time(s)	MI	MI-Bef	MI-Aft	Time(s)	CR	MI-Aft	Time(s)	CR	MI-Aft	Time(s)	CR
1	0.45	0.78	14	752.3	323.7	769.9	25	0.78	678.1	183	0.75	553.3	12	0.65
2	0.44	0.82	13	717.1	264.2	708.6	24	0.8	684.3	262	0.80	524.3	18	0.71
3	0.45	0.82	14	762.0	295.9	770.6	23.2	0.82	702.1	383.23	0.81	551.6	15	0.7
4	0.44	0.8	13.2	780.0	295.0	870.2	23.5	0.83	672.4	254	0.76	564.0	10	0.69
5	0.47	0.74	14.7	726.8	330.2	773.9	25	0.76	701.8	138	0.74	600.8	13	0.68
6	0.5	0.78	14.4	810.2	334.4	820.5	24.6	0.78	747	338	0.75	594.6	14	0.67
7	0.5	0.74	14.5	698.0	286.9	688.0	23	0.73	693.7	103	0.75	499.5	12.8	0.65
8	0.5	0.73	14.4	660.9	290.2	692.8	21	0.74	623.6	125	0.71	501.8	10	0.64
9	0.42	0.74	14.6	685.1	275.6	672.7	24	0.71	578.2	163	0.68	459.3	10	0.6
10	0.42	0.67	14.2	576.9	233.5	593.8	23.4	0.67	512.9	296	0.64	403.1	15.2	0.56
$\mu$	0.45	0.76	14.1	<b>716.9</b>	292.9	<b>736.1</b>	23.6	0.76	<b>659.4</b>	224.5	0.73	<b>525.3</b>	13	0.65

**Table 3. Similarity measures computed for Sagittal view for noisy images**

Case #	Non-parametric method (Variational method)							Parametric method (MIRT)						
	CR			MI				MI(space=1)			MI(space=5)			
	CR-bef	CR-Aft	Time(s)	MI	MI-Bef	MI-Aft	Time(s)	CR	MI-Aft	Time(s)	CR	MI-Aft	Time(s)	CR
1	0.48	0.6	16.6	500.2	308.3	488.3	26	0.59	413.0	188	0.5	345.6	15.2	0.51
2	0.1	0.22	16.6	86.09	58.4	78.8	28	0.23	105.1	203	0.24	68.4	17.8	0.2
$\mu$	0.29	0.41	16.6	<b>293.145</b>	183.35	<b>283.55</b>	27	0.41	<b>259</b>	195.5	0.37	<b>207</b>	16.5	0.3

**Table 4. Similarity measures computed for Axial view for noisy images**

Case #	Non-parametric method (Variational method)							Parametric method (MIRT)						
	CR			MI				MI(space=1)			MI(space=5)			
	CR-bef	CR-Aft	Time(s)	MI	MI-Bef	MI-Aft	Time(s)	CR	MI-Aft	Time(s)	CR	MI-Aft	Time(s)	CR
1	0.2	0.4	18	203.9	112.1	198.3	17	0.4	206.7	360	0.4	156.5	16.8	0.35
2	0.1	0.43	18.2	491.9	255.5	462.5	9	0.3	453.5	156	0.62	348.6	15.3	0.54
$\mu$	0.15	0.41	18.1	<b>347.9</b>	183.8	<b>330.4</b>	13	0.35	<b>330.1</b>	258	0.51	<b>252.5</b>	16.05	0.4

## 4 Conclusions

In this paper an efficient implementation of variational registration method was applied to MR and FMR images of spine. The method is based on curvature registration formulated in spatial domain. Two similarity measures; correlation ratio and mutual information were used and results were compared with the results of the MIRT toolbox. It was shown that for human spine images the variational non-parametric registration method produces better results in terms of accuracy and time compared to parametric methods for both similarity measures. Also it was shown that for noisy FMR spine images better registration results are produced when CR is used as the similarity measure.

As the future work, the implementation of variational method for registration of MR and FMR images are applied to 3D human spine images and the results will be compared with the results of parametric methods.

## Competing Interests

Authors have declared that no competing interests exist.

## References

- [1] Rueckert D, Aljabar P. Non-rigid registration using free-form deformations. *Medical Imaging, IEEE Transactions*. 2015;18 (8):712-721.
- [2] Sotiras A, Davatzikos C, Paragios N. Deformable medical image registration: A survey. *IEEE Transactions on Medical Imaging*. 2013;32(7):1153–1190.
- [3] Maes F, Loeckx D, Vandermeulen D, Suetens P. Image registration using mutual information. *Medical Imaging, IEEE Transactions*. 2003;91(10):1699 - 1722.
- [4] Prummera M, Horneggera J, Pfisterc M, Dorflerb A. Multi-modal 2D-3D non-rigid registration, *medical imaging 2006: Image Processing, Proc. of SPIE*. 2006;6144:61440X.
- [5] Rueckert D, et al. Non rigid registration using free-form deformations: Application to breast MR images. *IEEE Trans. Med. Imaging*. 1999;18:712–721.
- [6] Alvar-Gin'és Legaz-Aparicio, Rafael Verd'u-Monedero, Jorge Larrey-Ruiz, Fernando L'opez-Mir, Valery Naranjo, Angela Bernab'eu. Multimodal 3D Registration of Anatomic (MRI) and functional (fMRI and PET) Intra-patient Images of the Brain, *Artificial Computation in Biology and Medicine, of the series Lecture Notes in Computer Science*. 2015;9107:340-347.
- [7] Fischer B, Modersitzki J. A unified approach to fast image registration and a new curvature based registration technique. *Linear Algebra & its Applications*. 2004;308.
- [8] Andriy M. Non-rigid image registration: Regularization, algorithms and applications. Ph.D. thesis. Oregon Health & Science University; 2010.
- [9] Jhimli Mitra, Zoltan Kato, Robert Martí, Arnau Oliver, Xavier Lladó, Désiré Sidibé, Soumya Ghose, Joan Vilanova, Josep Comet, Fabrice Meriaudeau. A spline-based non-linear diffeomorphism for multimodal prostate registration. *Medical Image Analysis*. 2012;16:1259–1279.
- [10] Maes F, Collignon A, Vandermeulen D, Marchal G, Suetens P. Multimodality image registration by maximization of mutual information. *IEEE Transactions on Medical Imaging*. 1997;16(2):187-198.

- [11] Wells WM, Viola P, Atsumi H, Nakajima S. Multi-modal volume registration by maximization of mutual information. *Medical Image Analysis*. 1996;1(1):35-51.
- [12] Abhishek Singh, Ying Zhu and Christophe Chef d'hotel. A variational approach for optimizing quadratic mutual information for medical image registration. *Speech and Signal Processing (ICASSP)*. 2012 IEEE International Conference. 2012;557-560.
- [13] Edgar Arce-Santana, Daniel U. Campos-Delgado, Flavio Viguera-Gómez, Isnardo Reducindo, Aldo R. Mejía-Rodríguez. Non-rigid multimodal image registration based on the expectation-maximization algorithm. Klette R, Rivera M, Satoh S. (Eds.): *PSIVT 2013, LNCS 8333*. 2014;36-47.
- [14] Roche A, Malandain G, Pennec X, Ayache N. The correlation ratio as a new similarity measure for multimodal image registration. In: Wells WM, Colchester A, Delp SL. (eds.) *MICCAI 1998*. LNCS, Springer, Heidelberg. 1998;1496:1115-1124.
- [15] Alexis Roche, Grégoire Malandain, Xavier Pennec, Nicholas Ayache. The correlation ratio as a new similarity measure for multimodal image registration. *Proceedings MICCAI'98*. LNCS. 1998; 1496:1115{1124}.
- [16] Jan Modersitzki. *Numerical methods for image registration*.

---

© 2016 Sabaghian et al.; This is an Open Access article distributed under the terms of the Creative Commons Attribution License (<http://creativecommons.org/licenses/by/4.0>), which permits unrestricted use, distribution, and reproduction in any medium, provided the original work is properly cited.

**Peer-review history:**

The peer review history for this paper can be accessed here (Please copy paste the total link in your browser address bar)  
<http://sciedomain.org/review-history/14503>